25

Parametric and Robust Optimization Study of a Vibration Absorber with a Generalized Cubic, Quadratic and Non Integer Nonlinearities of Damping and Stiffness

M.–Lamjed Bouazizi[1] and S. Ghanmi[1] and R. Nasri[2]
[1]*Preparatory Engineering Institute (IPEIN), University of 7 November, 8000 M'rezgua –Nabeul,*
[2]*Research Unity of Materials Engineering, National Engineering School of Tunis, University of Tunis El Manar, BP37,1002 Le Belvedere Tunis, Tunisia*

1. Introduction

In order to reduce the vibrations in the revolving machines and the structures in general, the dynamic absorbers are often used in different mechanical and civil applications (Crankshaft, rotor of the wings of a helicopter, beams, etc).
The absorber is a mechanical oscillator called auxiliary system and it's added to the main vibrating structure, in order to carry out a transfer of energy from the main system to the auxiliary system. This latter can either be added on the main system, or directly envisaged in design.
A linear model is often insufficient to describe correctly the dynamical behaviour of a system, and then it's natural to introduce non linear structure models. To solve these non linear problems, iterative numerical algorithms are often used.
In order to approach the non linear dynamic behaviour of mechanical systems, many methods were proposed in the literature. As for the mechanical systems assimilated to a single dof system, one can mentioned different works. Whiston [1] studied the linear response of a mechanical oscillator with a single dof preloaded and subjected to a harmonic excitation. Natsiavas [2] studied the response of a vibration absorber applied to a machine with a nonlinear cubic stiffness of the Duffing type. In this chapter, numerical results are given with many parameter combinations. This leads to the improvement of the vibration absorber. The stability response, for periodic motion of harmonically excited single dof linear system with piecewise linear characteristics was studied by Natsiavas [3]. Chung et al.[4] carried out the extension of the method of incremental perturbation on a strongly nonlinear non-autonomous oscillator.
Concerning the discrete systems with several dof, many works were interested in the nonlinearity. Vakakis and Paipetic [5] studied the effect of the absorber viscosity on a conservative system with several dof. Optimal values for the parameters describing the behaviour of the absorber are determined. Natsiavas [6] discussed the response of a strongly

nonlinear system with several dof where the absorber is modeled by a linear spring and a residual force. Natsiavas and Tratskas [7] have studied a system with two nonlinear dof in translation and rotation motions by multi-scale method in time. Verros and Natsiavas [8] studied an oscillator with two dof with a cubic stiffness nonlinearity subjected to a harmonic charge. For this purpose, they used the perturbation method in order to study the effect of the parameters on the stability of the periodic solution. Zhu et al. [9] have studied a discrete two dof system with two cubic nonlinearities of stiffness and damping subjected to a harmonic excitation. They have used the method of the variation of the constant in order to obtain the periodic, quasi periodic and chaotic motions. Erkus [10] has accomplished a comparative study of the various numerical techniques of resolution for nonlinear structures, based on Newmark schema. Roy and Kumar [11] presented a method of multi-stage transverse linearization applied to a nonlinear dynamic system. El Bessiouny [12] studied effect of the quadratic and cubic nonlinearity of an elastomer shock absorber used in the torsion vibrations in an internal combustion engine. The stability of the solution is studied according to nonlinear terms. The multi-scale method was used in this work.

The majority of the optimization problems are of multi-objective nature. For their resolutions, there are several approaches of evolutionary algorithm. Schaffer [13] proposed an extension of a standard Genetic Algorithm to a modified one called Vector Evaluated Genetic Algorithm "VEGA".

Zitzler and Thiele [14] proposed a multi-objective optimization method which uses the concept of Pareto to compare the solutions. Srivinas and Deb [15] proposed an evolutionary algorithm of NSGA type (Not dominated Sorting Genetic Algorithms) based on the concept of Pareto dominance.

This chapter is based on the paper of Bouazizi et al.[16]. Firstly a two dof mechanical system composed of a one dof main system and a one dof absorber of vibration is proposed. The case of non integer power non linearity is considered also in this work in order to show the difference with integer cases.

The global system comprises generalized nonlinear stiffness and shock absorbers (cubic non linearity combined with a higher or lower power nonlinearities: 2,4 and 1.5) with a given proportioning.

For the resolution the unconditionally stable Newmark iterative scheme is used.

Here, one can seem for the non linear forces in the main system and in the absorber according to displacements and system trajectory in order to study the influence of some parameters and the type of non linearity.

Finally, the errors curves are found witch make it possible to conclude about the speed of convergence of the model compared to the importance of results.

A parametric study of the system as well as of the load and nonlinearities are carried out.

Secondly, the presence of uncertainties on the design parameters of a system can influence the results of the used models. Thus, one can use a robust multi-objective optimization methodology with respect to uncertainties on the design parameters. This methodology will be applied to a mechanical system comprising an absorber of vibration and equipped with nonlinearities of stiffness and damping of cubic, quadratic and non entire. This mixing of one of the two last nonlinearities with the cubic case constitutes our generalized non linearity.

The step of multi-objective optimization consists in seeking the first Pareto front of several linear and nonlinear objective functions by using genetic algorithm "NSGA ". Those make it possible to find the optimal nonlinear displacements.

The obtained solution guarantees the acceptable compromise of optimality/robustness. The robustness function is then introduced as supplementary objective function to each cost function Bouazizi et al. [16], Ghanmi et al. [17] and Ait Brik et al [18].

2. Basic equations

2.1 Introduction

One can consider a mechanical system called main system brought back to only one dof. An absorber with only one dof is assembled on this system. The main system is characterized by a mass m_1, a linear spring of stiffness k_1, a linear shock absorber or damping c_1, two stiffness nonlinearities of respectively $k_1^{'}$ with variable power r and $k_1^{''}$ cubic and two other similar nonlinearities of damping with the two respective coefficients of nonlinearities $c_1^{'}$ and $c_1^{''}$. It is subjected to a harmonic load of variable amplitude and fixed pulsation ω corresponding approximatively to the natural pulsation of the main system. The mechanical characteristics of the absorber are similar to those of the main system with index 2 instead of 1. The absorber parameters are then: m_2, k_2, c_2, $k_2^{'}$, $k_2^{''}$, $c_2^{'}$ and $c_2^{''}$.

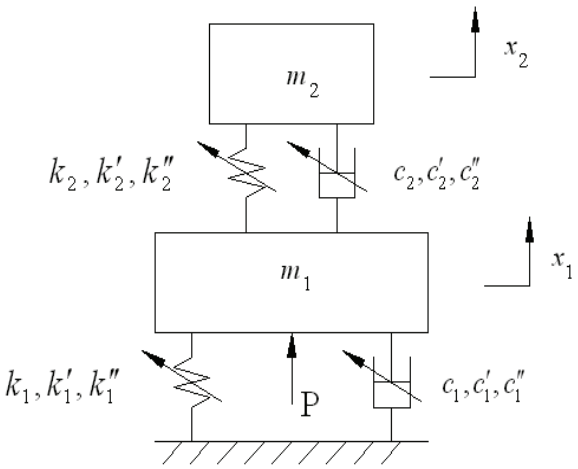

Fig. 1. Basic model

Figure 1 presents the global system of study. x_1 is defined as the absolute vertical displacement of the mass m_1 and x_2 is the vertical displacement of the mass m_2 relatively to the mass m_1.

2.2 Analytical formulation

From the Lagrange method, the equations of motion for the system can be rearranged as follows:

$$\begin{aligned} &(m_1+m_2)\ddot{x}_1 + m_2\ddot{x}_2 + f_1(x_1) + R_1(x_1) = P_0\cos\omega t \\ &m_2\ddot{x}_1 + m_2\ddot{x}_2 + f_2(x_2) + R_2(x_2) = 0 \end{aligned} \tag{1}$$

where:

$f_i(x_i) = k_i x_i + k_i^{'} x_i^r + k_i^{''} x_i^3$, $(i = 1,2)$, are the generalized stiffness nonlinear forces.

$R_i(x_i) = c_i \dot{x}_i + c_i^{'} x_i^{r-1} \dot{x}_i + c_i^{''} x_i^2 \dot{x}_i$, $(i = 1,2)$, are the generalized damping nonlinear forces.

Further, the nonlinear force on a mass m_i is referred to as the addition of the two nonlinear forces mentioned previously.

The positive real parameter r is introduced in order to consider various situations of nonlinearities i.e.:

- $r = 1$ or $r = 3$: cubic nonlinearity.
- $r = 2$: quadratic nonlinearity superposed to cubic nonlinearity.
- $r = 1.5$: non integer nonlinearity superposed to cubic nonlinearity.

These last three situations constitute what we call generalized nonlinearity.

The equations of motion (1) can be written in a matrices form:

$$[M]\{\ddot{u}\} + [C_{nl}]\{\dot{u}\} + [K_{nl}]\{u\} = \{F\} \tag{2}$$

where:

$\{u\} = \begin{Bmatrix} x_1 \\ x_2 \end{Bmatrix}$, $\{\dot{u}\} = \begin{Bmatrix} \dot{x}_1 \\ \dot{x}_2 \end{Bmatrix}$, $\{\ddot{u}\} = \begin{Bmatrix} \ddot{x}_1 \\ \ddot{x}_2 \end{Bmatrix}$ and $\{F\} = \begin{Bmatrix} P_0 \cos \omega t \\ 0 \end{Bmatrix}$ are respectively the displacement, velocity, acceleration and external force vector, and $[M] = \begin{bmatrix} m_1 + m_2 & m_2 \\ m_2 & m_2 \end{bmatrix}$,

$[C_{nl}(u)] = \begin{bmatrix} c_1 + c_1^{'} x_1^{r-1} + c_1^{''} x_1^2 & 0 \\ 0 & c_2 + c_2^{'} x_2^{r-1} + c_2^{''} x_2^2 \end{bmatrix}$ and

$[K_{nl}(u)] = \begin{bmatrix} k_1 + k_1^{'} x_1^{r-1} + k_1^{''} x_1^2 & 0 \\ 0 & k_2 + k_2^{'} x_2^{r-1} + k_2^{''} x_2^2 \end{bmatrix}$

are respectively the mass, nonlinear damping and nonlinear stiffness matrix. Further, adimensional writing is used by carrying out the following changes of variables:

$$\begin{aligned}
&x_{sta} = \frac{P_0}{k_1}, \quad \omega_1^2 = \frac{k_1}{m_1}, \bar{x}_1 = \frac{x_1}{x_{sat}}, \\
&\bar{x}_2 = \frac{x_2}{x_{sat}}, \quad \bar{m}_2 = \frac{m_2}{m_1}; \bar{k}_2 = \frac{k_2}{k_1}, \\
&\bar{k}_i^{'} = \frac{k_i^{'}}{k_i} x_{sta}^{(r-1)}, \quad \bar{k}_i^{''} = \frac{k_i^{''}}{k_i} x_{sta}^2, \\
&\bar{c}_i^{'} = \frac{c_i^{'}}{c_i} x_{sta}^{(r-1)}, \bar{c}_i^{''} = \frac{c_i^{''}}{c_i} x_{sta}^2 \quad (i = 1,2).
\end{aligned} \tag{3}$$

$$[\bar{M}]\{\ddot{\bar{u}}\} + [\bar{C}_{nl}(\bar{u})]\{\dot{\bar{u}}\} + [\bar{K}_{nl}(\bar{u})]\{\bar{u}\} = \{\bar{F}\} \tag{4}$$

After dividing with ($k_1 x_{sta}$), the equation of motion (2) becomes:

where:

$\{\bar{u}\} = \begin{Bmatrix} \bar{x}_1 \\ \bar{x}_2 \end{Bmatrix}$, $\{\dot{\bar{u}}\} = \frac{1}{\omega_1}\begin{Bmatrix} \dot{\bar{x}}_1 \\ \dot{\bar{x}}_2 \end{Bmatrix}$, $\{\ddot{\bar{u}}\} = \frac{1}{\omega_1^2}\begin{Bmatrix} \ddot{\bar{x}}_1 \\ \ddot{\bar{x}}_2 \end{Bmatrix}$ and $\{\bar{F}\} = \begin{Bmatrix} \cos\omega t \\ 0 \end{Bmatrix}$ are respectively the displacement, velocity, acceleration and external force adimensional vector.

$\left[\bar{M}\right] = \begin{bmatrix} 1+\bar{m}_2 & \bar{m}_2 \\ \bar{m}_2 & \bar{m}_2 \end{bmatrix}$, $\left[\bar{C}_{nl}(\bar{u})\right] = 2\begin{bmatrix} \alpha_1(1+\bar{c}_1'\bar{x}_1^{(r-1)}+\bar{c}_1''\bar{x}_1^2) & 0 \\ 0 & \alpha_2\sqrt{\bar{k}_2\bar{m}_2}(1+\bar{c}_2'\bar{x}_2^{(r-1)}+\bar{c}_2''\bar{x}_2^2) \end{bmatrix}$

and $\left[\bar{K}_{nl}(\bar{u})\right] = \begin{bmatrix} 1+\bar{k}_1'\bar{x}_1^{(r-1)}+\bar{k}_1''\bar{x}_1^2 & 0 \\ 0 & \bar{k}_2(1+\bar{k}_2'\bar{x}_2^{(r-1)}+\bar{k}_2''\bar{x}_2^2) \end{bmatrix}$ are respectively the mass, the nonlinear damping and the nonlinear stiffness adimensional matrix.

α_1 and α_2 are respectively the damping ratio of the main system and the absorber.

For the numerical resolution, we need the nonlinear terms of the main system $(\bar{k}_1', \bar{k}_1'', \bar{c}_1', \bar{c}_1'')$, nonlinear terms of the auxiliary system (absorber) $(\bar{k}_2', \bar{k}_2'', \bar{c}_2', \bar{c}_2'')$ and basic terms $\bar{m}_2, x_{sta}, \omega_1, \alpha_1, \alpha_2$ and $\bar{k}_2$.

The initial conditions are given by :

$$\{\bar{u}(0)\} = \begin{Bmatrix} \bar{x}_{10} \\ \bar{x}_{20} \end{Bmatrix},\ \{\dot{\bar{u}}(0)\} = \frac{1}{\omega_1}.\begin{Bmatrix} \dot{\bar{x}}_{10} \\ \dot{\bar{x}}_{20} \end{Bmatrix} \text{ and } \{\bar{F}(0)\} = \begin{Bmatrix} 1 \\ 0 \end{Bmatrix}.$$

The beginning of computation, we start by the computation of the initial acceleration:

$$\{\ddot{\bar{u}}(0)\} = \begin{Bmatrix} \ddot{\bar{x}}_{10} \\ \ddot{\bar{x}}_{20} \end{Bmatrix} = \left[\bar{M}\right]^{-1}\left\{-\left[\bar{C}_{nl}(0)\right]\{\dot{\bar{u}}(0)\} - \left[\bar{K}_{nl}(0)\right]\{\bar{u}(0)\} + \{\bar{F}(0)\}\right\} \tag{5}$$

The resolution of equation (4) can be obtained by a numerical integration with using the unconditionally stable Newmark scheme.

At the step n where $t = n.\Delta t$ (Δt is the time integration step), the equation (4) can be written:

$$\left[\bar{M}\right]\{\ddot{\bar{u}}_n\} + \left[\bar{C}_{nl}(\bar{u}_n)\right]\{\dot{\bar{u}}_n\} + \left[\bar{K}_{nl}(\bar{u}_n)\right]\{\bar{u}_n\} = \{\bar{F}_n\} \tag{6}$$

where: the index n corresponds to the value in n^{th} step.

The Newmark scheme consists in approximating the adimensional displacement and velocity vectors as follows:

$$\begin{aligned} \{\bar{u}_{n+1}\} &= \{\bar{u}_n\} + \Delta t.\omega_1\{\dot{\bar{u}}_n\} + \frac{\Delta t^2}{2}.\omega_1^2[(1\text{-}2\beta)\{\ddot{\bar{u}}_n\} + 2\beta\{\ddot{\bar{u}}_{n+1}\}] \\ \{\dot{\bar{u}}_{n+1}\} &= \{\dot{\bar{u}}_n\} + \Delta t.\omega_1\,[(1\text{-}\gamma)\{\ddot{\bar{u}}_n\} + \gamma\{\ddot{\bar{u}}_{n+1}\}] \end{aligned} \tag{7}$$

The accuracy and the stability of this scheme depends on the values of the two parameters β and γ. In our simulation, we used the habitual parameters ($\gamma = \frac{1}{2}$, $\beta = \frac{1}{4}$) corresponding to the called average acceleration method (unconditionally stable scheme).

The process consists in defining the indicators $\{\tilde{u}_{n+1}\}$ and $\{\dot{\tilde{u}}_{n+1}\}$ according to the terms known at the moment $t = n.\Delta t$ while taking $\{\ddot{\bar{u}}_{n+1}\} = \{0\}$:

$$\begin{aligned} \{\tilde{u}_{n+1}\} &= \{\bar{u}_n\} + \Delta t\ \omega_1 \{\dot{\bar{u}}_n\} + \frac{\Delta t^2}{2}\omega_1^2\ [(1\text{-}2\beta)\{\ddot{\bar{u}}_n\}] \\ \left\{\dot{\tilde{u}}_{n+1}\right\} &= \{\ddot{\bar{u}}_n\} + \Delta t.\omega_1[(1\text{-}\gamma)\{\ddot{\bar{u}}_n\}] \end{aligned} \tag{8}$$

One can define the residual equation (Res) as a function of $\{\bar{u}_{n+1}\}$ at the moment $t_{n+1} = (n+1)\Delta t$ as following:

$$\text{Res}(\{\bar{u}_{n+1}\}) = \left[\bar{M}\right]\{\ddot{\bar{u}}_{n+1}\} + \left[\bar{C}(\bar{u}_{n+1})\right]\{\dot{\bar{u}}_{n+1}\} + \left[\bar{k}(\bar{u}_{n+1})\right]\{\bar{u}_{n+1}\} - \{\bar{F}_{n+1}\} = \{0\} \tag{9}$$

The nonlinear equation (9) can be solved in an iterative way by the method of Newton-Raphson in the following way.
Let $\{\bar{u}^k_{n+1}\}$, $\{\dot{\bar{u}}^k_{n+1}\}$ and $\{\ddot{\bar{u}}^k_{n+1}\}$) respectively the approximation of adimensional displacement, velocity and acceleration vector obtained in the k^{th} iteration of the time step t_{n+1}. Those can be corrected, for the next iteration, respectively in the form:

$$(\{\bar{u}^k_{n+1}\} + \{\Delta\bar{u}_{n+1}{}^k\}, \{\dot{\bar{u}}^k_{n+1}\} + \{\Delta\dot{\bar{u}}_{n+1}{}^k\}, \{\ddot{\bar{u}}^k_{n+1}\} + \{\Delta\ddot{\bar{u}}_{n+1}{}^k\}).$$

The end of the iteration cycle is carried out, when the residue of displacement falls below a certain precision level initially fixed.
In the numerical simulation (section 3), several cases will be study.
In the first time, two particular cases, the cubic nonlinear stiffness (Duffing type) and the cubic nonlinear damping (Van Der Pol type), are studied.
In the second time, the mixed of the previous cubic nonlinear cases (damping and stiffness) is considered.
Finally, the mixed generalized nonlinearity cases (power 2 "quadratic" and cubic, and power 1.5 and cubic) are studied.

3. Simulation results and discussion

In this section, we are interested in first part to the vibratory behaviour of the global two dof system through the representation of the following curves:

- $X_1(t)$: Displacement of the main system (1) according to time,
- $X_2(t)$: Relative displacement between the absorber (2) and the main system according to time,
- $V_1(X_1)$: Phase diagram of the main system 1,
- $V_2(X_2)$: Phase diagram of the absorber,
- $NL-F1$: Nonlinear force 1 of the system (1) according to X_1,
- $NL-F2$: Nonlinear force 2 of the absorber according to X_2,
- $X_2(X_1)$: System trajectory,

- ε : Relative error on displacement after convergence (limit fixed at 10^{-6}) according to time.

These curves are given for the four indicated nonlinearity cases mentioned above.

In second part, one is interested in optimization of the absorber by seeking its linear and nonlinear optimal characteristics: $\bar{k}_2$, $\bar{k}_2^{'}$, $\bar{k}_2^{''}$ *et* $\bar{m}_2$ with minimization of the maximum nonlinear displacement $X_1(t)$.

The non dimensional results are converted finally in physics results when the displacement and the velocity are multiplied by (x_{sta}) in (m) also the velocity well be in m/s.

The curves give only the non dimensional results and need to be converted are mentioned.

In this section, we will take for computation convenience and practical considerations: $\bar{m}_2 = 0.01$, $x_{sta} = 0.05\, m$, $\omega_1 = 70\ rad/s$, $\Delta t = 3.10^{-4}\, s$, $\bar{k}_2 = 0.01$ and $\alpha_1 = \alpha_2 = 0.001$.

It is noted that the excitation pulsation is selected close to the natural pulsation of the main system witch is experimented in another submitted paper. The absorber is the used only in the resonance domain in this work.

The time step is chosen to have a good convergence.

With a less step time we find the same results.

The initials conditions are equal to zero but when we modify them the results don't change

3.1 Cubic nonlinear stiffness (Duffing case)

The nonlinear mechanical characteristics of the system are: $\bar{k}_1^{'} = \bar{k}_1^{''} = \bar{k}_2^{'} = \bar{k}_2^{''} = 250$ and $\bar{c}_1^{'} = \bar{c}_1^{''} = \bar{c}_2^{'} = \bar{c}_2^{''} = 0$. It should be noted that the absolute physical characteristics in this case, have the value ($\frac{k_1^{'}}{k_1} = \frac{k_1^{''}}{k_1} = \frac{k_2^{'}}{k_2} = \frac{k_2^{''}}{k_2} = 10^5$) in international system (SI).

Figure 2a illustrates the nonlinear responses in displacements of the main system (dof 1) and of the absorber (dof 2). It is noted that the main system vibrations are weaker than those of the absorber.

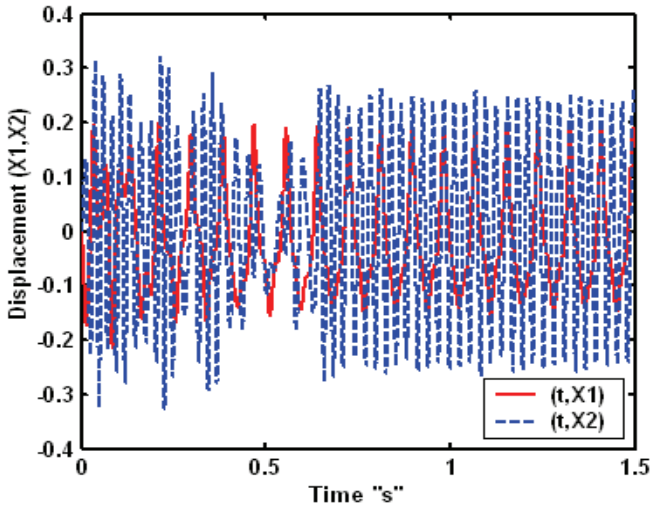

Fig. 2a. Nonlinear temporal responses "Duffing case"

After a transitory period of time, one notes a more regular vibration for the absorber and a phenomenon of periodic vibration for the main system and the absorber but with different periods. The period of the main system is similar to that of the force excitation but that of the absorber is about three times lower then the precedent period.
Figure 2b illustrates the two phase curves corresponding to the Duffing case where attractors are visible only for the main system but for the absorber we note a limit cycle orbit after the transitory period.

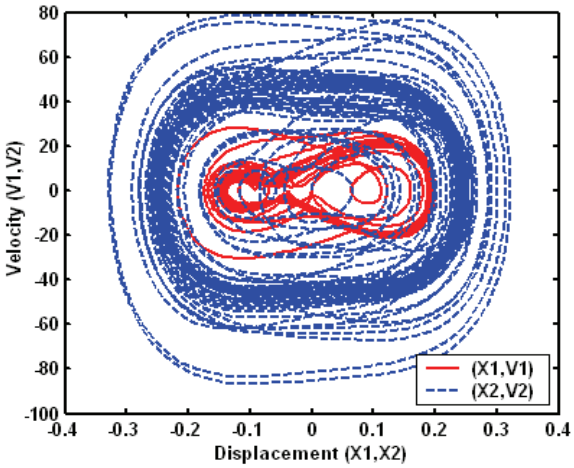

Fig. 2b. Phase diagrams "Duffing case"

The figure 3 a and b illustrate the nonlinear forces on each mass according to corresponding displacement. One notes a hysteretic cubic cycle, and an inflection point corresponding to the steady balance point.

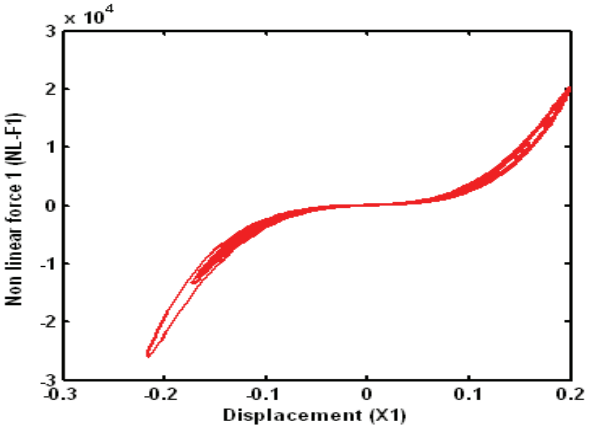

Fig. 3a. Nonlinear forces: (X1, NL-F1) "Duffing case"

This hysteresis has a low width caused by the weak linear damping; it is more visible for the absorber. In the same way the cubic form of the nonlinear force is more visible for the absorber than for the main system. One notes also the appearance of a narrow level stretch around the stable point especially for the main system.

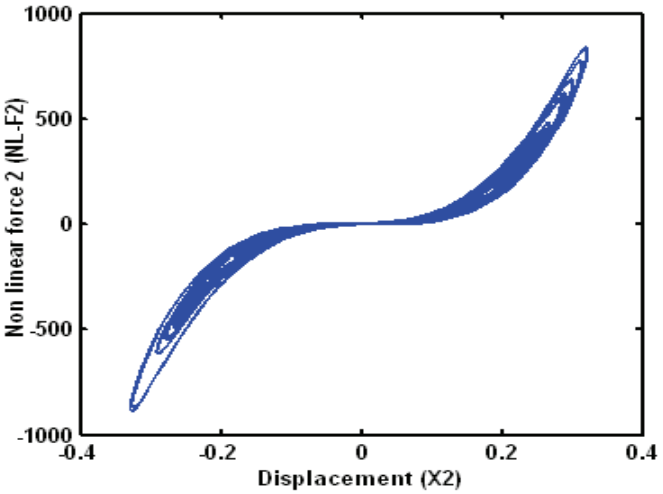

Fig. 3b. Nonlinear forces: (X2, NL-F2) "Duffing case"

Figure 4a illustrates the very complex trajectory of the global system in the plan (X_1, X_2) for these proportioning.

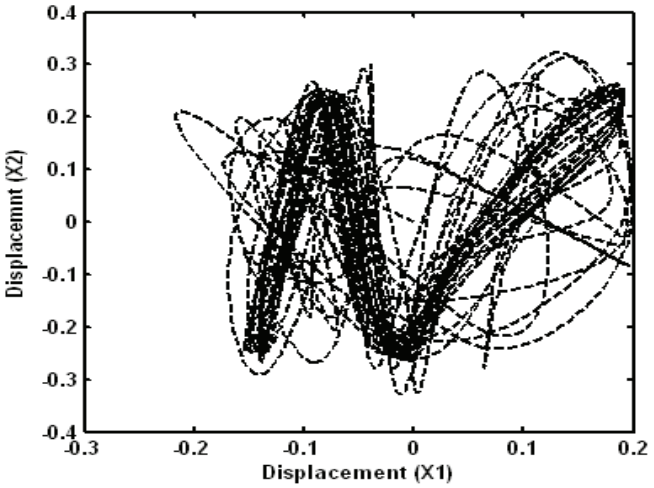

Fig. 4a. System trajectory in the plan (X1, X2) "Duffing case"

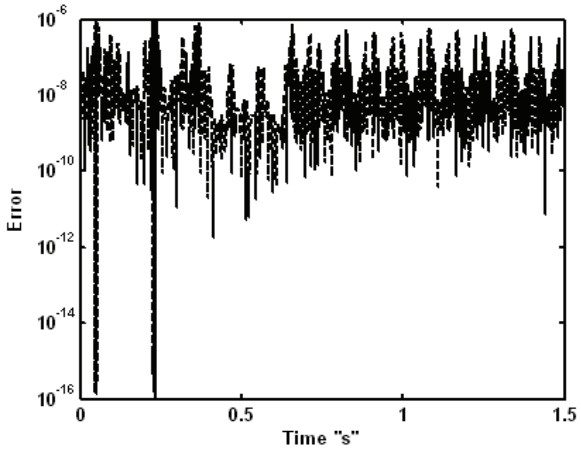

Fig. 4b. Error curve "Duffing case"

Figure 4b shows the relative error curve of displacement. It is noted that the errors are satisfactory compared to the selected limit (10^{-6}) during the iterative process, which proves a good convergence for the selected model and parameters.

3.2 Cubic nonlinear damping (Van Der Pol case)

The nonlinear mechanical characteristics of the system are: $\overline{k}_1^{'} = \overline{k}_1^{''} = \overline{k}_2^{'} = \overline{k}_2^{''} = 0$ and $\overline{c}_1^{'} = \overline{c}_1^{''} = \overline{c}_2^{'} = \overline{c}_2^{''} = 250$. It should be noted that the absolute physical characteristics in this case, have the value ($\frac{c_1^{'}}{c_1} = \frac{c_1^{''}}{c_1} = \frac{c_2^{'}}{c_2} = \frac{c_2^{''}}{c_2} = 10^5$) in international system (SI) and also these parameters are selected among several tests, guaranteeing useable results on the one hand and of good convergence on the other hand.

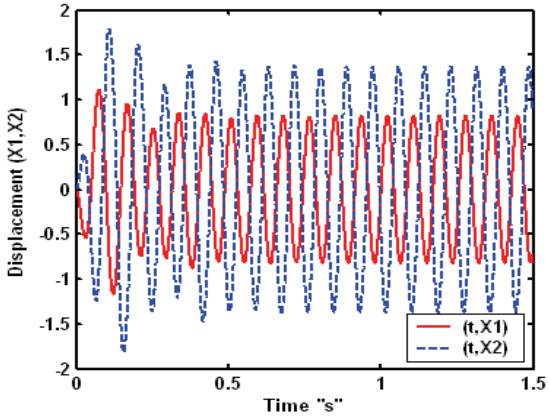

Fig. 5a. Nonlinear temporal responses "Van Der Pol case"

Figure 5a illustrates the responses in displacements of the main system and of the absorber. It is noted that the responses of the two dof are practically harmonic and in phase opposition, in which the pulsation is close to that of excitation. The behaviour resembles for this case and after a transitory period to that of a linear system. The absorber causes a notably decrease for the vibrations of the main system.

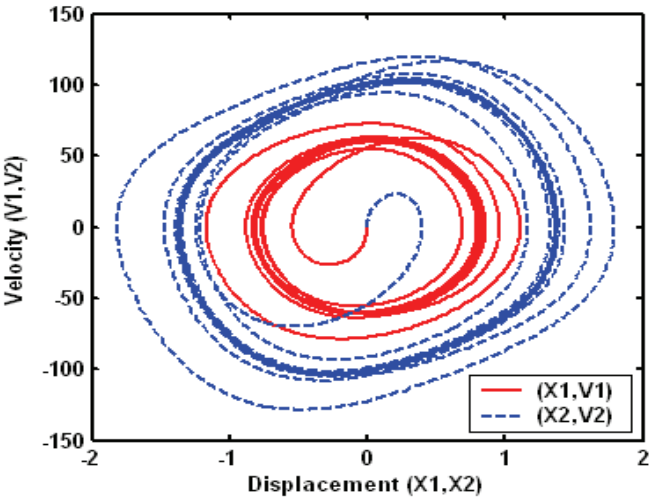

Fig. 5b. Phase diagrams "Van Der Pol case"

Consequently, the phase diagram for each dof (figure 5b) indicates a cycle limit meaning stability, these two cycles are complementary.

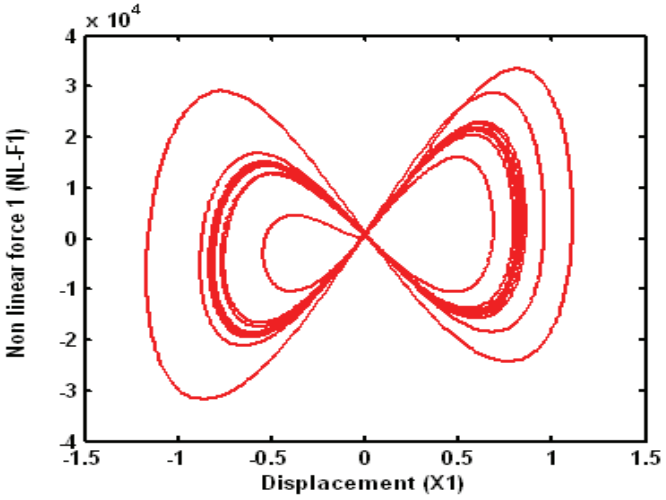

Fig. 6a. Nonlinear forces: (X1, NL-F1) "Van Der Pol case"

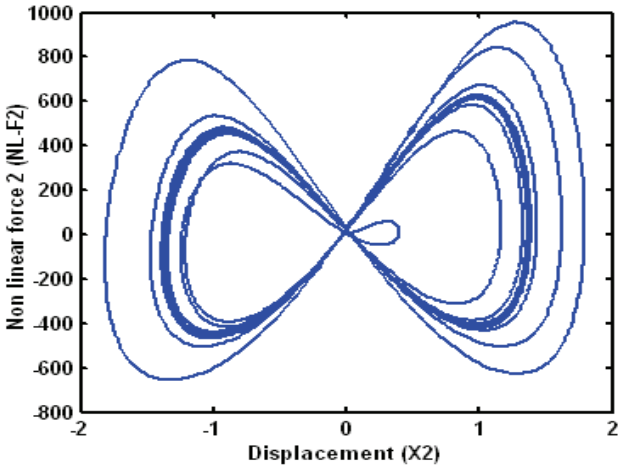

Fig. 6b. (X2, NL-F2) "Van Der Pol case"

The figure 6 a and b illustrate the nonlinear forces exerted on each mass according to corresponding displacement. One notes a broad opening hysteresis caused by strongly nonlinear damping for each dof. It is practically symmetrical compared to the steady balance position. It is also noted that the forces evolve in phase opposition for the two dof as well as the displacements.

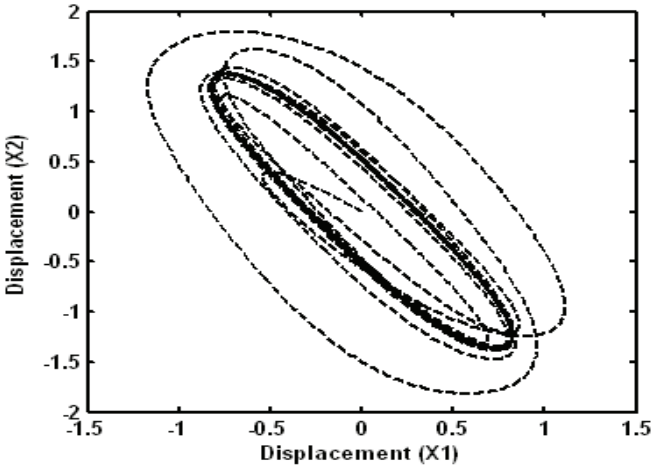

Fig. 7a. System trajectory in the plan (X1, X2) "Van Der Pol case"

Figure 7a illustrates a quasi periodic and elliptic stable trajectory of the global system in the plan (X_1, X_2). Figure 7b shows the relative error curve. It is noted that the errors are close to 10^{-6} during the iterative process, which proves a difficult convergence compared to the Duffing case for the selected model and parameters. If one continues to increase the damping proportioning, convergence becomes difficult.

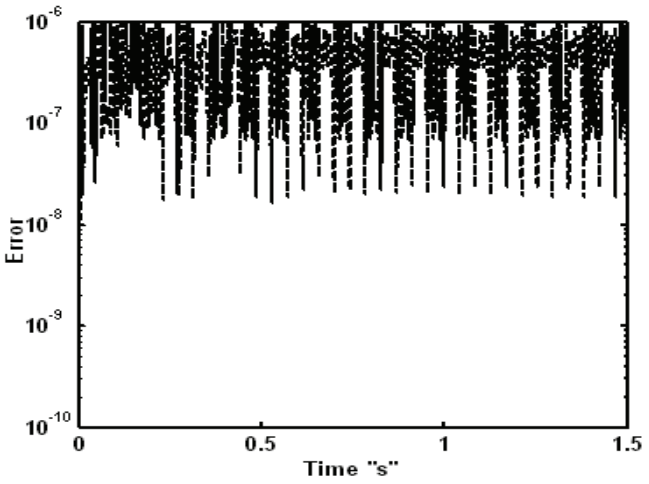

Fig. 7b. Error curve "Van Der Pol case"

3.3 Cubic nonlinear damping and stiffness: $r = 3$

In this subsection and for all that will follow, we consider mixed (damping and stiffness) non linearity cases. The nonlinear mechanical characteristics of the system are: $\overline{k}_1' = \overline{k}_1'' = \overline{k}_2' = \overline{k}_2'' = 250$ and $\overline{c}_1' = \overline{c}_1'' = \overline{c}_2' = \overline{c}_2'' = 250$. This choice respects the same nonlinear damping and stiffness proportioning previously used in (3.1) and (3.2) subsections.

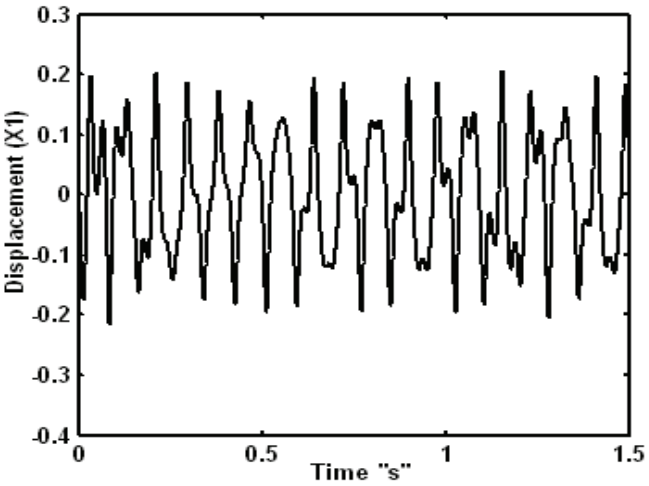

Fig. 8a. Nonlinear response (X1(t)) "Cubic damping and stiffness case"

The figure 8 a and b illustrate the response in time (a) and phase diagram (b) of the main system. One observes the strongly nonlinear behaviour in the temporal curve. We note also

the presence of two attractors more visibly that for the Duffing case and synonymous with a predominance of the stiffness non linearity. For the absorber, there is no notable modification compared to the Duffing case, in spite of the non validity of the superposition principle.

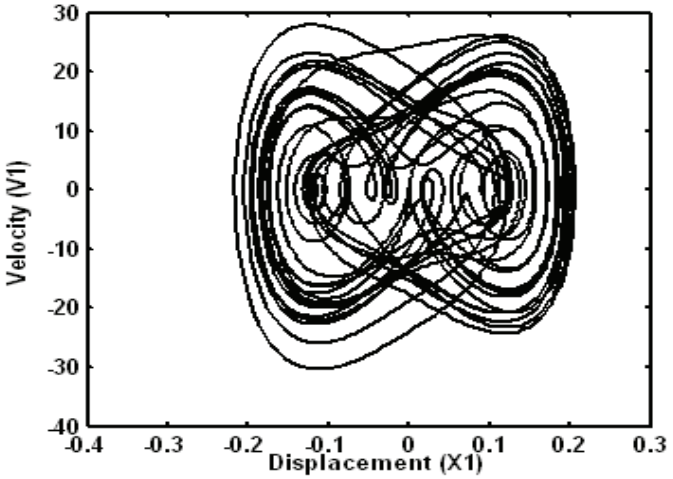

Fig. 8b. Phase diagram (X1,V1) "Cubic damping and stiffness case"

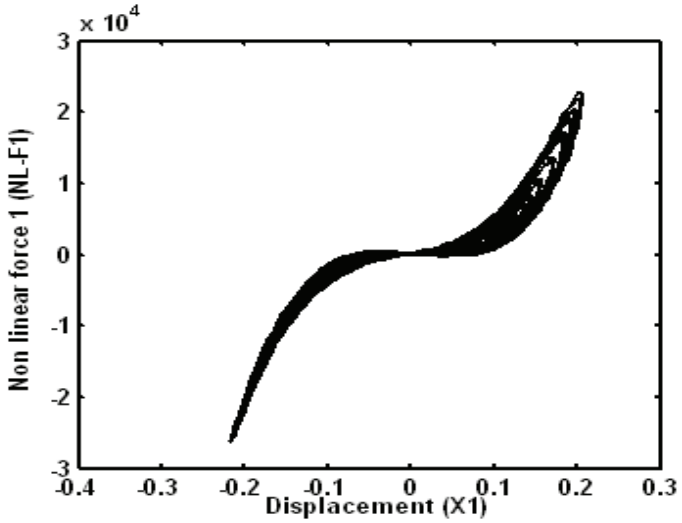

Fig. 9a. Nonlinear forces (X1, NL-F1) "Cubic damping and stiffness case"

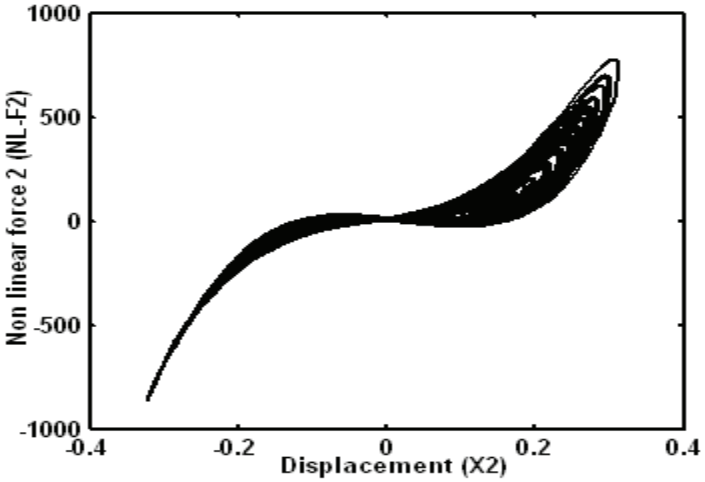

Fig. 9b. Nonlinear forces (X2, NL-F2) "Cubic damping and stiffness case"

The figure 9 a and b illustrate the nonlinear forces applied on each mass according to corresponding displacement. A low width cubic hysteretic cycle is observed for the main system but it's broader for the absorber, this may be caused by nonlinear damping. This width cycle form is dissymmetric between the two sides.

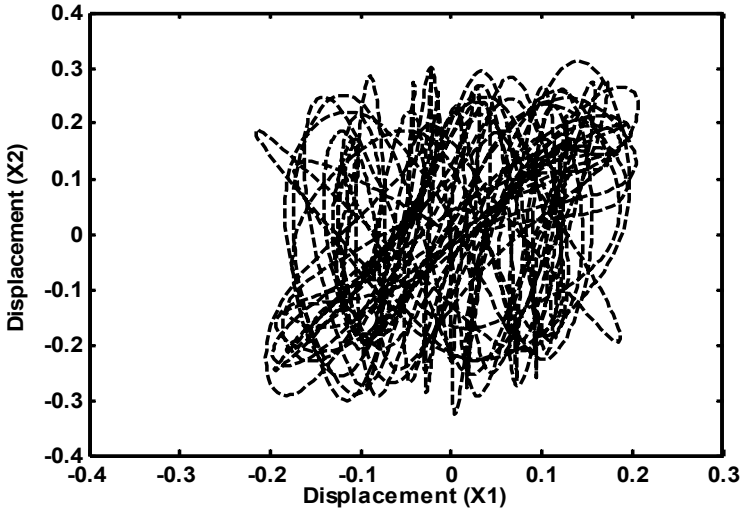

Fig. 10a. System trajectory in the plan (X1, X2) "Cubic damping and stiffness case"

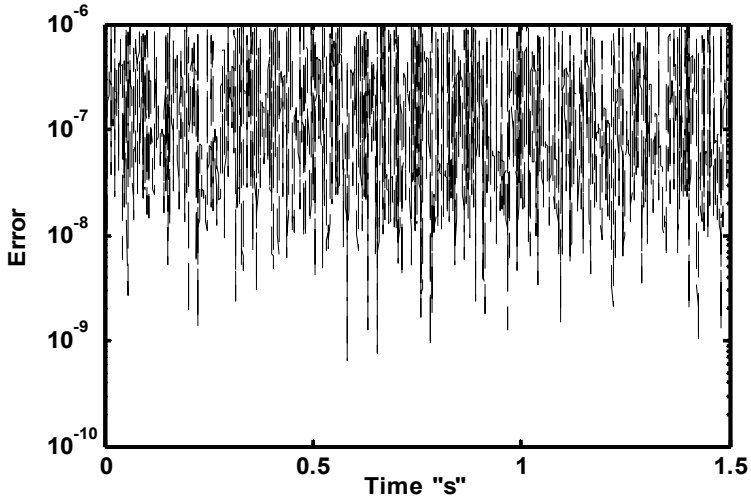

Fig. 10b. Error curve "Cubic damping and stiffness case"

It's also noted than the nonlinear forces are more affected by stiffness than by damping in form and amplitude. The narrow level stretch around the stable point disappears in this case. In the same way the nonlinear force of the main system is dominant. Figure 10a illustrates the complex trajectory of the global system in the plan (X1, X2), synonymous of instability but less than the Duffing case.

Fig. 10b shows the relative error curve. It is noted that the errors are dispersed between 10^{-9} and 10^{-6} during the iterative process, which doesn't prove a fast convergence for such high amounts.

We can conclude in this subsection that in the cubic damping and stiffness case, there are two attractors which appear clearly only when the amplitude of the excitation force increases. The strongly non linear damping may be the cause of this phenomenon.

The nonlinear hysteresis force curve is much more significant when the amplitude of the exciting force increases.

This hysteresis is not symmetric around the inflection point corresponding to the steady balance position.

Noticeable level stretch in the vicinity of this position, especially, for high loads is observed.

3.4 Nonlinear generalized damping and stiffness case: $r = 2$

In this section, the nonlinear generalized case (quadratic and cubic) in stiffness and damping is studied. The nonlinear mechanical system characteristics are: $\overline{k}_1^{'} = \overline{k}_2^{'} = \overline{c}_1^{'} = \overline{c}_2^{'} = 5$ and $\overline{k}_1^{''} = \overline{k}_2^{''} = \overline{c}_1^{''} = \overline{c}_2^{''} = 0.25$. It should be noted that the absolute physical characteristics in this case, have the same value ($\frac{k_1^{'}}{k_1} = \frac{k_1^{''}}{k_1} = \frac{c_1^{'}}{c_1} = \frac{c_1^{''}}{c_1} = 10^2$) in SI and also these parameters are selected among several tests, guaranteeing useable results on the one hand and of good convergence on the other hand.

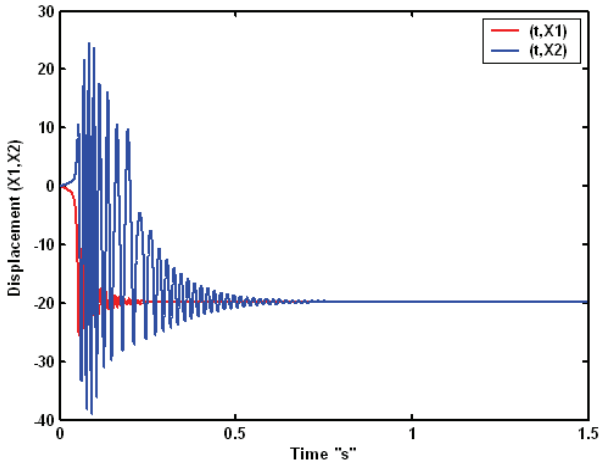

Fig. 11. Temporal nonlinear responses: (X1(t) and X2(t)) "Generalized case: quadratic and cubic for week damping"

Figure 11 shows the evolution of displacements of both dof according to time. It is noted that the absorber strangles completely the vibration in this proportioning configuration. If we increase the proportioning non linearity practically all the vibrations of the main system disappear. Moreover, as the global movement is very much diminished from t=0.6s. This is one of the effects of this generalized nonlinearity case. The displacement of the main system oscillates while remaining of negative sign, before converging quickly towards a constant value, the vibration is almost eliminated. However, absorber oscillates between the two signs before converging towards the same limit as that of the main system.

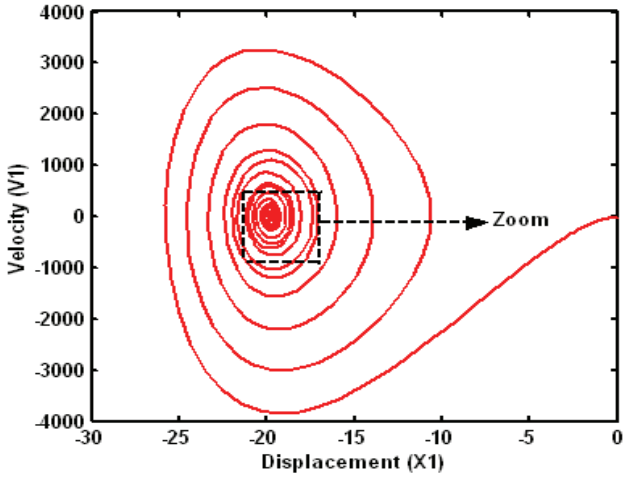

Fig. 12a. Phase diagram (X1,V1) "Generalized case: quadratic and cubic"

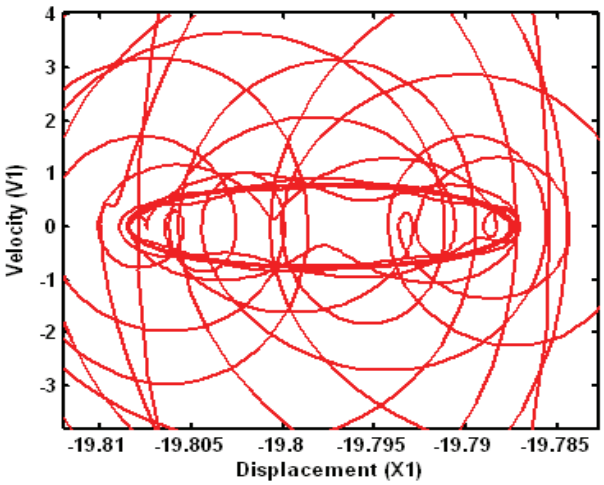

Fig. 12b. Zoom on the attractors "Generalized case: quadratic and cubic"

Figure 12a illustrates the phase diagram of the main system and shows the existence of two very close attractors, clarified by zoom (figure 12b). The latter indicates an elliptic orbit whose focuses coincide with the attractors.

Figure 13a illustrates the phase diagram of the absorber and also shows the existence of two very close attractors, clarified by zoom (figure 13b). Furthermore, an elliptic orbit is observed whose focuses coincide with the attractors.

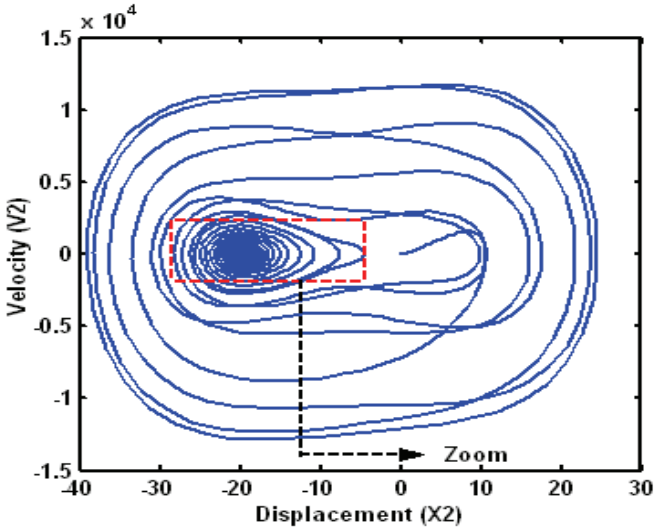

Fig. 13a. Phase diagram (X2,V2) "Generalized case: quadratic and cubic for week damping"

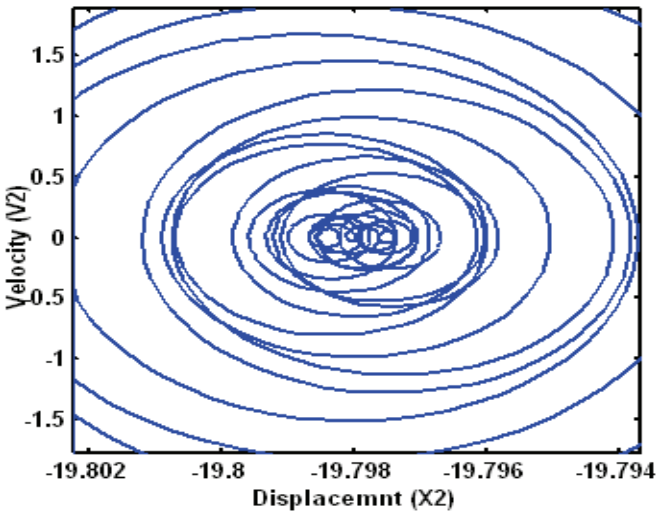

Fig. 13b. Zoom on the attractors "Generalized case: quadratic and cubic for week damping"

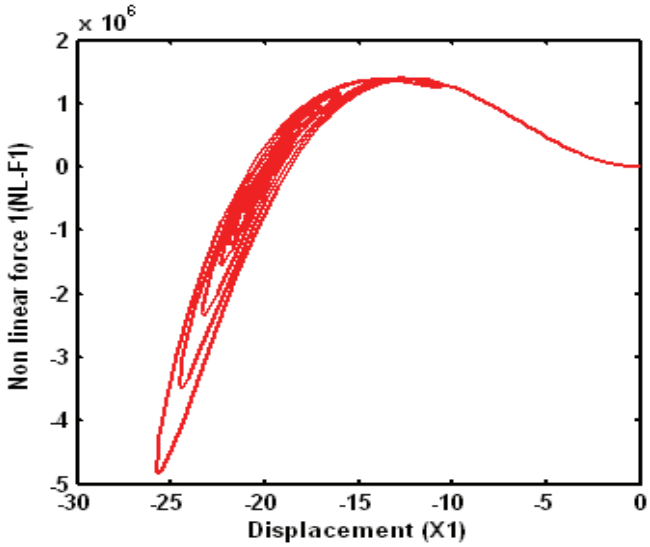

Fig. 14a. Nonlinear forces (X1, NL-F1) "Generalized case: quadratic and cubic for week damping"

The figure 14 a and b illustrate the applied nonlinear forces on each mass according to corresponding displacement. It's noted for the main system has a dominant parabolic form corresponding to a half hysteresis cycle at critical point with null force.

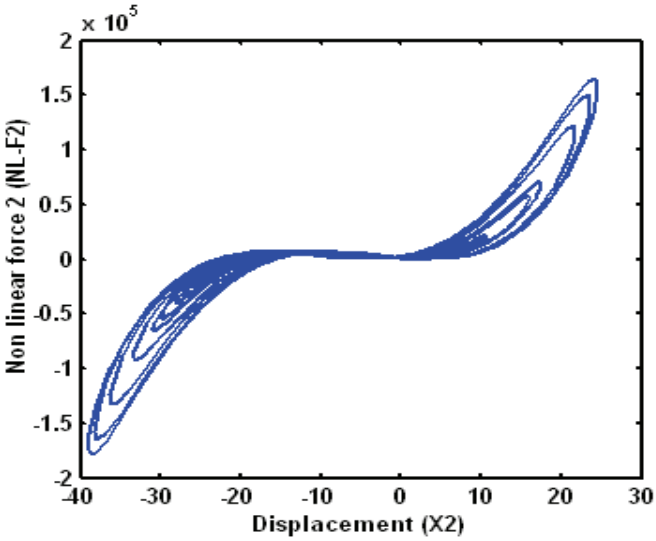

Fig. 14b. Nonlinear forces (X2, NL-F2) "Generalized case: quadratic and cubic for week damping"

This is more visible in figure 14a. But, a cubic hysteresis cycle with average width appears for the absorber, caused by nonlinear damping.
In the same way the amplitude of the nonlinear force of the main system is dominant. Also, the hysteresis opening is more significant for the absorber.

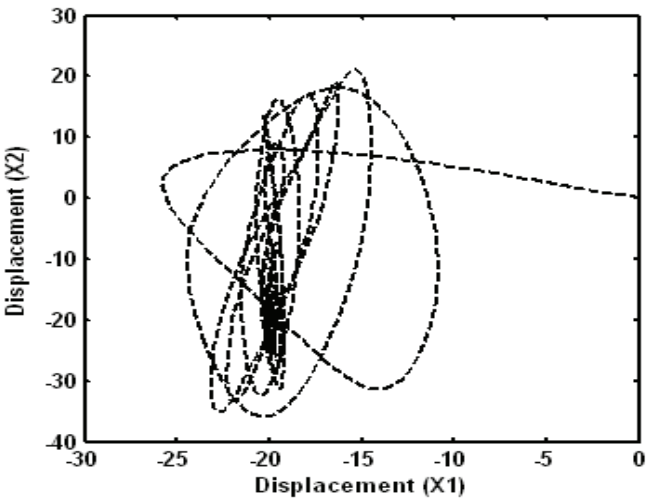

Fig. 15a. System trajectory in the plan (X1, X2) "Generalized case: quadratic and cubic for week damping"

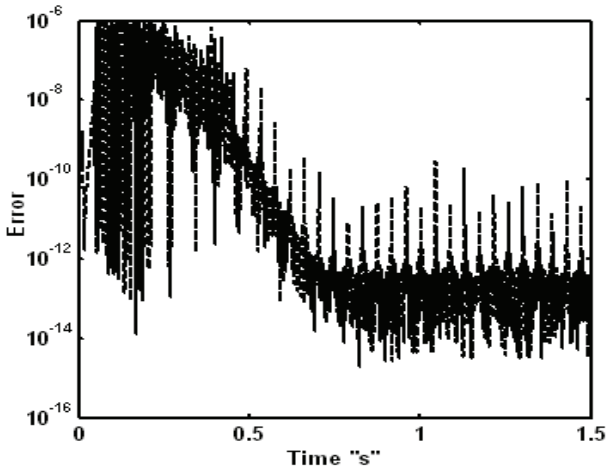

Fig. 15b. Error curve "Generalized case: quadratic and cubic for week damping"

Figure 15a illustrates the global system complex trajectory in the plan (X_1, X_2). It is quickly convergent to a critical point which differs notably from the steady balance position.
Figure 15b shows the curve of relative error. It is noted that the errors are dispersed, with a difficult convergence at the beginning but it becomes very fast after a certain time close to t=0.6s.

- ***Effect of the proportioning coefficients in this generalized case*** ($r = 2$)

The nonlinear mechanical characteristics of the system are: $\overline{k}_1^{'} = \overline{k}_2^{'} = 5$; $\overline{k}_1^{''} = \overline{k}_2^{''} = 0.25$ and $\overline{c}_1^{'} = \overline{c}_2^{'} = 500$; $\overline{c}_1^{''} = \overline{c}_2^{''} = 25$. In this case, it should be announced that we multiplied all the physical damping coefficients by 100 whereas we maintained those of stiffness.

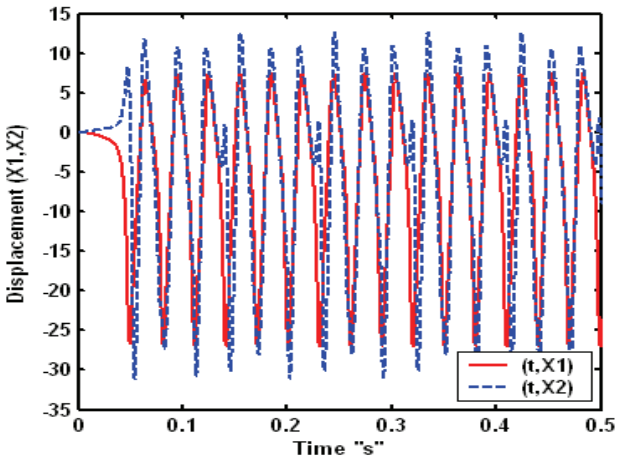

Fig. 16a. Nonlinear temporal responses (X1(t) and X2(t)) "Generalized case: quadratic and cubic for strongly damping"

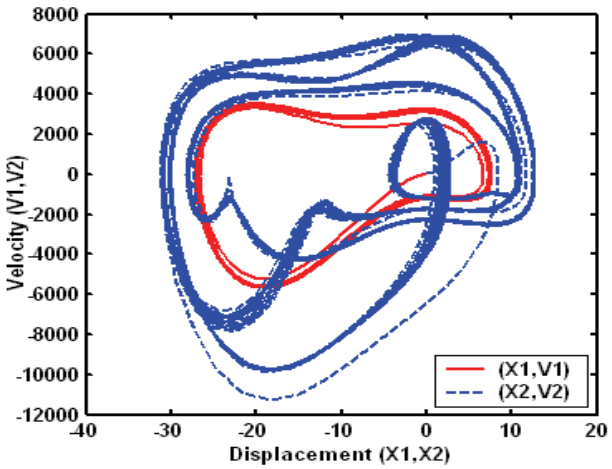

Fig. 16b. Phase diagrams "Generalized case: quadratic and cubic for strongly damping"

Figure 16a shows the displacements variation of both dof according to time. It is noted that the absorber is not the best adapted for this proportioning. The movement of the main system is similar then for linear behaviour, whereas that of the absorber takes a strongly nonlinear form.

Figure 16b illustrates the phase curves for the two dof. It is noted that when the damping proportioning of the absorber increases the main system has an elliptic limit cycle, whereas the absorber attractors persist converging with two limits cycle.

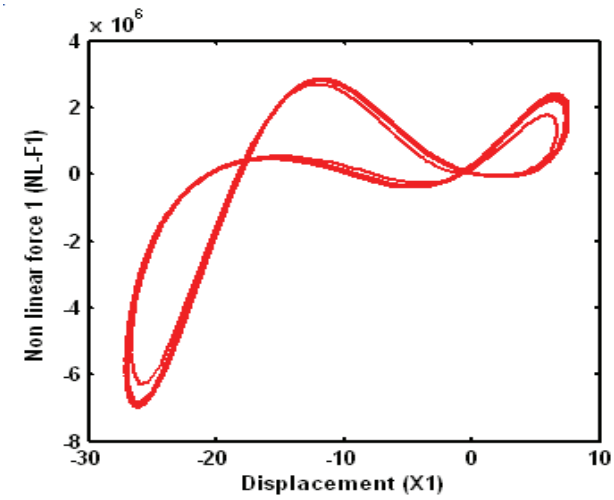

Fig. 17a. Nonlinear forces: (X1, NL-F1) "Generalized case: quadratic and cubic for strongly damping"

The figure 17 a and b show the variations of the nonlinear forces according to respective displacement.

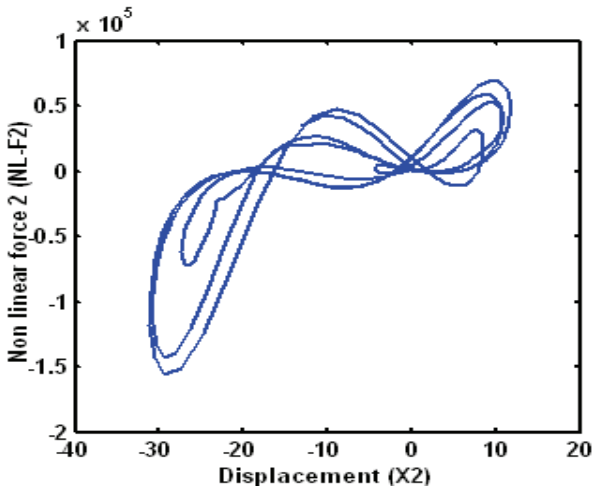

Fig. 17b. Nonlinear forces (X2, NL-F2) "Generalized case: quadratic and cubic for strongly damping"

It is noted that the increase in the damping proportioning creates a third hysteretic cycle of parabolic form for small displacements at the two critical points. One of these two points corresponds to the steady balance and the other corresponds to the extreme position of the absorber.

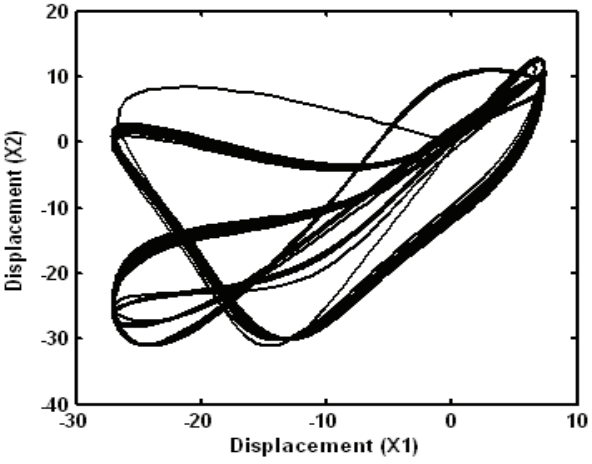

Fig. 18a. System trajectory in the plan (X1, X2) "Generalized case: quadratic and cubic for strongly damping"

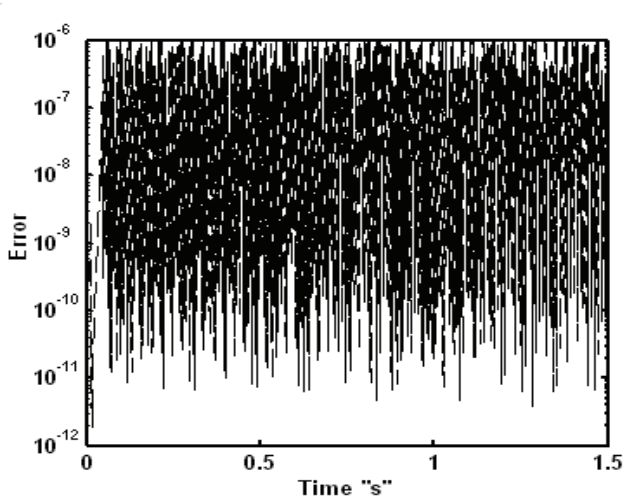

Fig. 18b. Error curve "Generalized case: quadratic and cubic for strongly damping"

Figure 18a illustrates the complex trajectory of the global system in the plan (X1, X2) but a stability is apparent with two complicate limit cycle orbits.

Figure 18b shows the curve of relative error. It is noted that the errors are dispersed between 10^{-12} and 10^{-6} during the iterative process, the convergence is better than previously and it does not change in time. Damping acts in the direction of vibration stabilization.

For this subsection, we can conclude that for this generalized case of non linearity the behaviour of the system is clearly different of the previously cases (subsections: 3.1, 3.2 and 3.3).

- The vibration of the main and the auxiliary system disappear relatively fast;
- The attractors are visible only with zooming;
- The hysteretic cycle of forces is original with a parabolic tendency and the apparition of one, two and three spindles.

These effects are strongly influenced by the proportioning of nonlinear parameters.

3.5 Nonlinear generalized damping and stiffness case: $r = 1.5$

In this section, the nonlinear generalized case (power 1.5 and cubic) in stiffness and damping is studied. The nonlinear mechanical system characteristics are: $\overline{k}_1^{'} = \overline{k}_2^{'} = \overline{c}_1^{'} = \overline{c}_2^{'} = 22.36$ and $\overline{k}_1^{''} = \overline{k}_2^{''} = \overline{c}_1^{''} = \overline{c}_2^{''} = 0.25$. It should be noted that the absolute physical characteristics in this case, have the same value ($\frac{k_1^{'}}{k_1} = \frac{k_1^{''}}{k_1} = \frac{c_1^{'}}{c_1} = \frac{c_1^{''}}{c_1} = 10^2$) in SI. These proportioning are decreased to make more quick the convergence and more significant physical results.

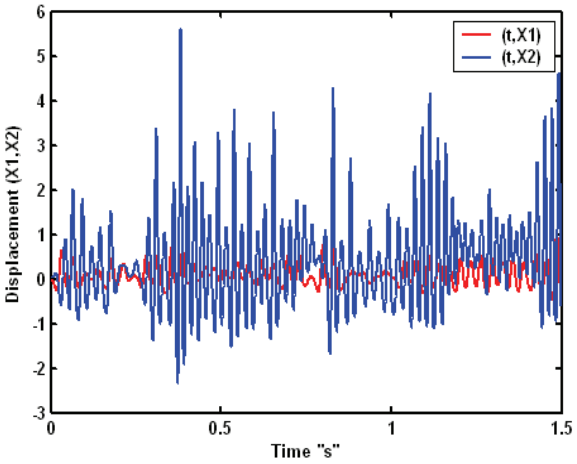

Fig. 19. Temporal nonlinear responses: (X1(t) and X(t)) "Generalized case: power 1.5 and cubic for week damping"

Figure 19 shows the displacements evolution for the two dof according to time. It is noted that the auxiliary system completely absorbs the vibration in this proportioning configuration. It is as to note as the movement is relatively irregular similar of specified non linearity. That may be one of the effects of the generalized non linearity for the non integer power less then 2.

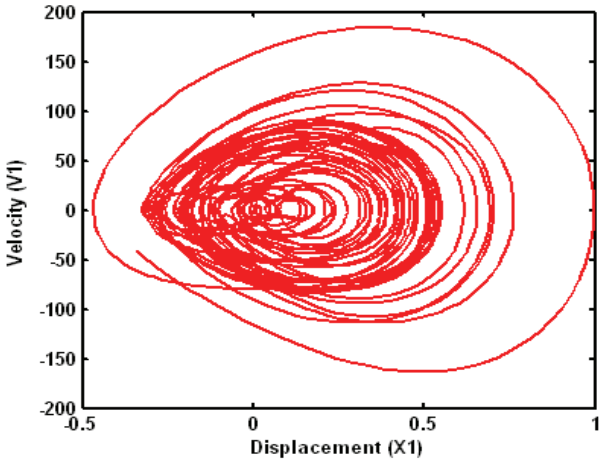

Fig. 20a. Phase diagrams (X1, V1) "Generalized case: power 1.5 and cubic for week damping"

The figure 20 a and b illustrate the phase curves of the main system and the absorber. They show the existence of two attractors very brought closer with an oval cycle orbit.

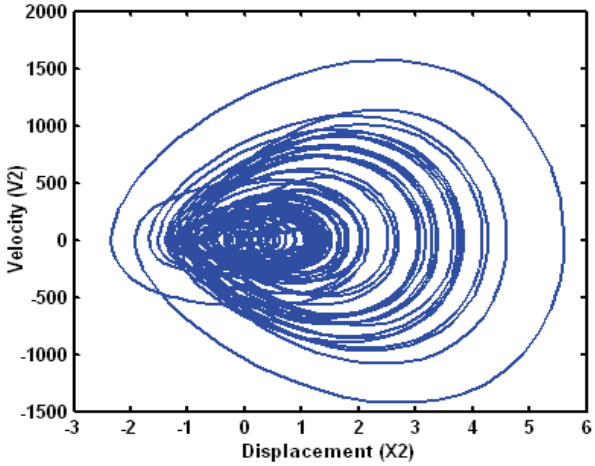

Fig. 20b. Phase diagrams (X2, V2) "Generalized case: power 1.5 and cubic for week damping"

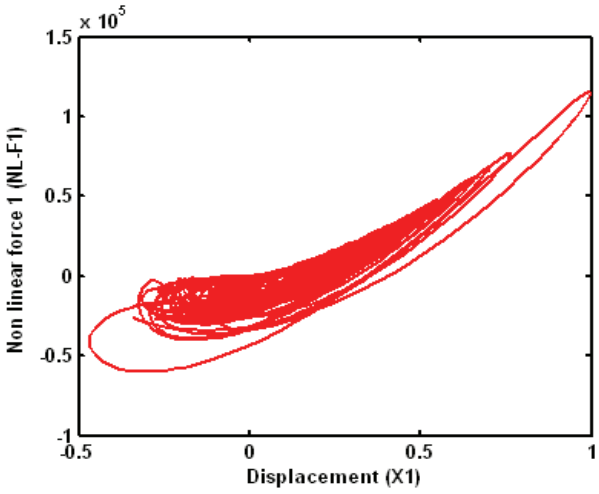

Fig. 21a. Nonlinear forces (X1, NL-F1) "Generalized case: power 1.5 and cubic for week damping"

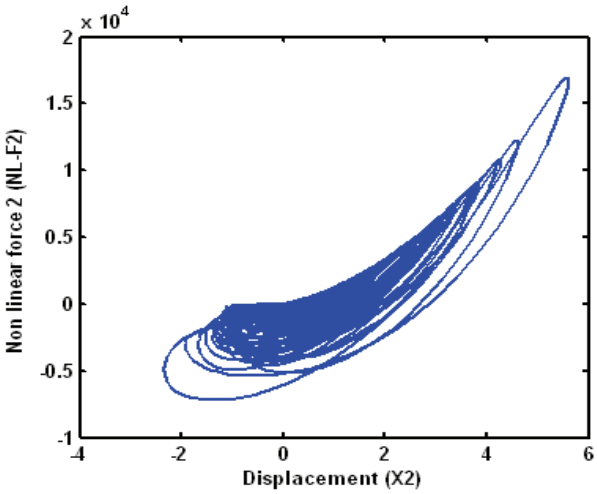

Fig. 21b. Nonlinear forces (X2, NL-F2) "Generalized case: power 1.5 and cubic for week damping"

The figure 21 a and b illustrate the nonlinear applied forces on each mass according to corresponding displacement. It is noted that for the two dof one has a dominant parabolic form with a fast convergence towards the steady balance with null forces. If one compares these results with the generalized quadratic case one notices a significant difference mainly for the absorber, which shows the originality of this case with a non integer power between 1 and 2.

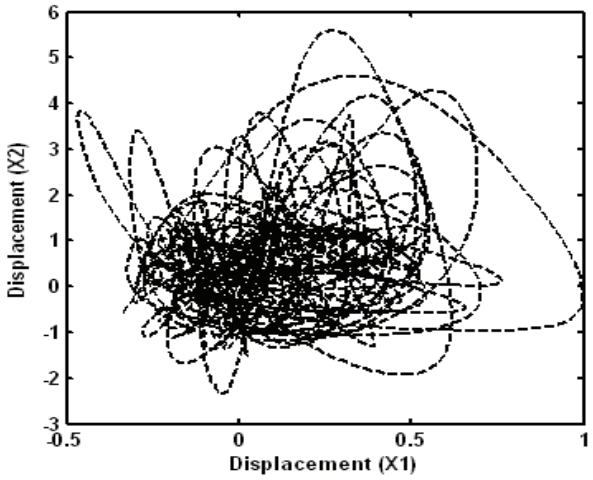

Fig. 22a. The trajectory of the system in the plan (X1, X2) "Generalized case: power 1.5 and cubic for week damping"

Figure 22a illustrates the global system complex trajectory in the plan (X_1, X_2). One notes a less regular trajectory with very difficult convergence as well as for the main system as for the

absorber. Figure 22b shows the curve of relative error. It is noted that the errors are dispersed between 10^{-9} and 10^{-6} during the iterative process, what proves an acceptable convergence.

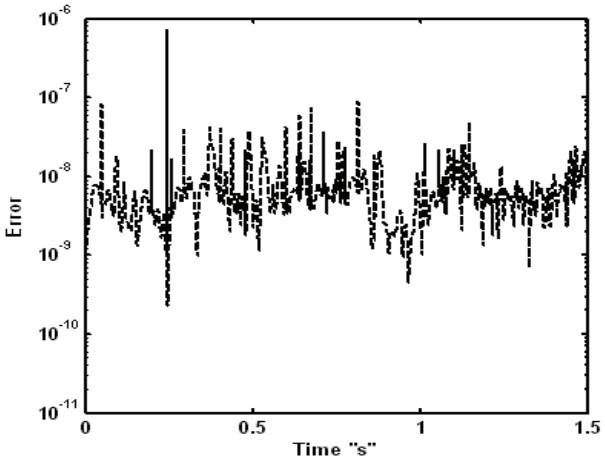

Fig. 22b. Error curve "Generalized case: power 1.5 and cubic for week damping"

- ***Effect of the proportioning coefficients in this generalized case*** ($r = 1.5$)

The nonlinear mechanical system characteristics are: $\overline{k}_1^{'} = \overline{k}_2^{'} = 22.36$; $\overline{k}_1^{''} = \overline{k}_2^{''} = 0.25$; and $\overline{c}_1^{'} = \overline{c}_2^{'} = 2236$; $\overline{c}_1^{''} = \overline{c}_2^{''} = 25$. In this case, we keep the stiffness constant and we multiplied those of damping by 100.

Figure 23 shows the variation of displacements of the two dof according to time.It is noted that the absorber is not the best adapted for this proportioning.

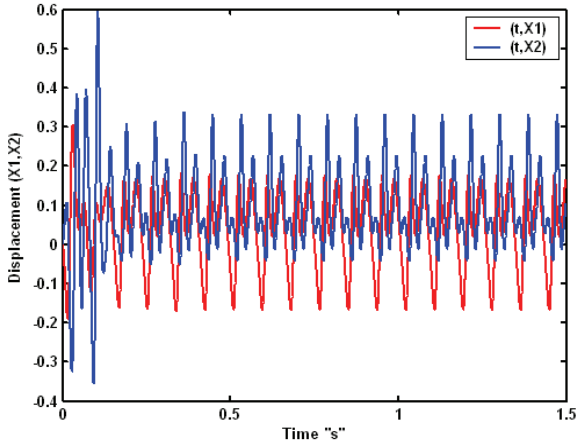

Fig. 23. Temporal nonlinear responses: (X1(t) and X2(t)) "Generalized case: power 1.5 and cubic for strongly damping"

It is also notable that the main system movement is similar to that of the absorber in amplitude but with a great dephasing. The form of these curves is strongly nonlinear but, after the transitory phase, the movement is periodic and it is stabilized by damping. The period of these motions is similar to that of excitation but with a high non linearity.
The figure 24 a and b illustrate the phase curves of the main system and the absorber. They especially show the existence of two limits cycle for the absorber. For the main system we observe only one limit cycle.

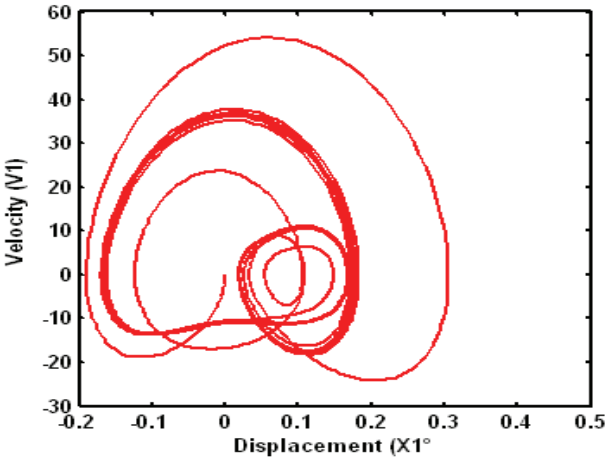

Fig. 24a. Phase diagrams (X1, V1) "Generalized case: power 1.5 and cubic for strongly damping"

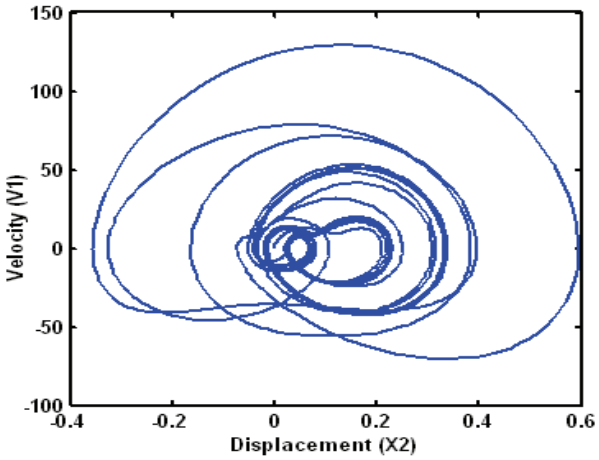

Fig. 24b. Phase diagrams (X2, V2) "Generalized case: power 1.5 and cubic for strongly damping"

The figure 25 a and b illustrate the nonlinear forces on each mass according to corresponding displacement. It is noted that for the two dof we observe more opened hysteretic form than the previous case with week damping.
Figure 26-a illustrates the complex trajectory of the global system in the plan (X1, X2). One notes a less regular trajectory with difficult convergence notably for the absorber.

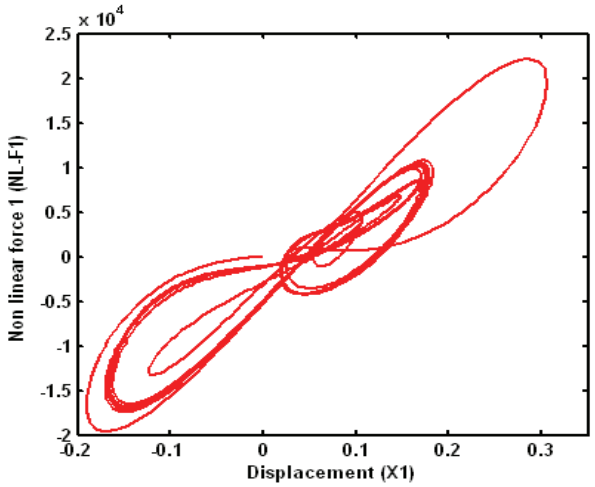

Fig. 25a. Nonlinear forces (X1, NL-F1) "Generalized case: power 1.5 and cubic for strongly damping"

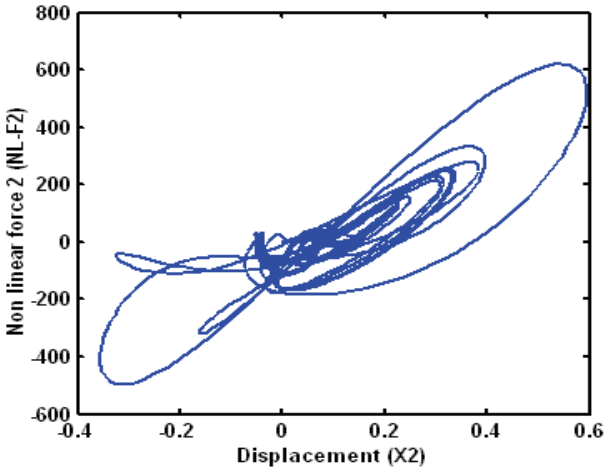

Fig. 25b. Nonlinear forces (X2, NL-F2) "Generalized case: power 1.5 and cubic for strongly damping"

Figure 26b shows the curve of relative error. The errors are dispersed between 10^{-8} and 10^{-6} during the iterative process, which proves difficulty of the convergence of this model compared to the case with a weak nonlinear damping. We can conclude:

- Increase the proportioning of the non linear damping of the system stabilizes the system vibration;
- The attractors become less visible with damping and the hysteretic cycle well be more symmetric around the steady balance position;
- The convergence is more difficult when the non linear damping increases.

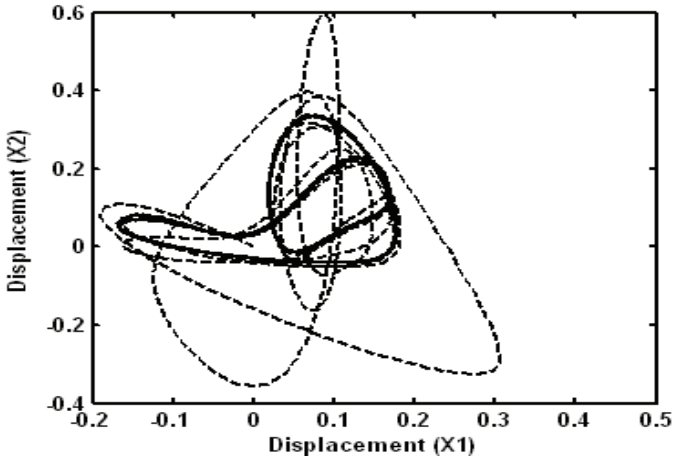

Fig. 26a. The trajectory of the system in the plan (X1, X2) "Generalized case: power 1.5 and cubic for strongly damping"

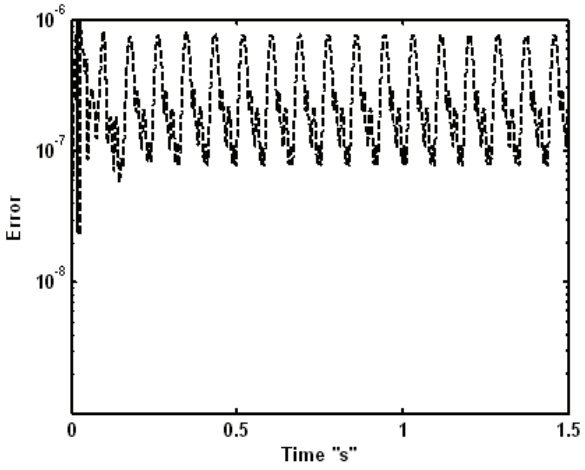

Fig. 26b. Error curve "Generalized case: power 1.5 and cubic for strongly damping"

Table 1. Recapitulation

Generalized case : r=1.5		Generalized case : r=2		Generalized case : r=3	Va
Strongly stiffness and damping	Strongly stiffness and Week damping	Strongly stiffness and damping	Strongly stiffness and Week damping	Strongly stiffness and damping	St da
- Periodic - Non linear	-Strongly irregular	-Non linear - Regular and periodic	- Quickly converge - Decreasing motion	Very irregular	-H - t op ph
- Complex limits of cycle	- Oval hidden 2 attractors	-2 limit cycles	2 attractors with zoom	2 visible attractors	- I of
- Open cubic cycle - Quickly convergent towards the steady balance	-Parabolic cycle	- 3 lobes of Hysteretic cycles-	Half of cycle with Critical point	-Cubic cycle -More open in one side	-C 2 s -B sy
- Irregular - Quickly convergent	- very Irregular	- Stable complex	Elliptic	Complex	El
- High iteration count - Difficult convergence	Week	-Low -Instable	Great then low after transition time	Intermediary	Gr
Hysteretic cycle changing tendency with displacement	-Good convergence - Cycle with week power and convergence point	Quadratic dominance for low displacement	Hysteretic cycle with Critical point	Dissymmetrical hysteretic cycle	Ba co

General comments:

To recapitulate one can include commenting the two first cases treated, witches are often mentioned in the literature.

Concerning the cubic damping and stiffness case (r=3), we note that for this model the non linearity of stiffness is rather dominant in spite of the strong amounts chosen for damping.

When one goes up in nonlinearity power beyond the power three, few changes appear on the nonlinear behaviour of the system for a week damping and a cycle with three spindles when the damping increases. For the last case the trajectory becomes more complicated.

When one interferes a non integer power nonlinearity (here power r=1.5) with cubic non linearity the convergence of computations becomes more difficult and it becomes even impossible for a rational between 2 and 3.

Indeed the attractors become closer to each other and only a zoom can separate them.

The appearance of half hysteretic cycle of nonlinear force at critical point is typical of this model.

Table 1 recapitulates these results.

4. Robust multi-objective optimization

The problems of optimization in the field of the machinery of the structures are often multi-objective; the latter can be in conflict. For that, it is necessary to choose a strategy of multi-objective optimization able to propose the best alternatives among several. A multi-objective optimization requires two steps witch is:

- Determination of the objective functions to be optimized

Obtaining these objective (or cost) functions are carried out directly during optimization by sampling.

- Choice of the technique of search for the optimal solutions

To search the optimal solutions, the genetic algorithm of NSGA type is used. Indeed, this algorithm makes it possible to better explore the design space and to exploit the whole of the Pareto front.

Generally, a problem of multi objective optimization is expressed by the equation below:

$$\min F(x)=\left(f_1(x), f_2(x),\ldots\ldots, f_n(x)\right)^T ; x \in S$$

where: $f_1(x), f_2(x),\ldots\ldots, f_n(x)$ are the cost functions and $x=\left(x_1, x_2,\ldots\ldots, x_n\right)^T$ is the vector of n parameters of optimization, $S \in R^n$ represents the whole of the realizable solutions and $F(x)$ is the vector of the functions to be optimized.

The whole of the optimal solutions is that formed by the solutions which are not dominated by others. The physical parameters used to describe a structure are often random. These parameters are generally identified like random variables and are introduced into an approach of resolution of the problems such as optimization. In the field of the optimization of the structures, the taking into account of the robustness of the solutions is essential in the research of the optimal design. In fact it is well-known that a theoretically excellent solution can prove to be catastrophic in practice if the errors made during manufacture for example do not make it possible to obtain the values of the variables of design with a sufficient

precision. A sub-optimal but stable solution with respect to the tolerances of manufacture can prove much more interesting for the originator.

Generally the construction of a robustness function is based on the mean value and the standard deviation. Indeed, many authors proposed to define the robustness function f^r of an original objective function *f* as being the relationship between the mean value and the standard deviation: $f^r = \left(\sigma_f / \mu_f\right)^{-1}$.

The ratio σ_f / μ_f indicates dispersion (or the vulnerability function $f^v(x)$) of *f*, where μ_f and σ_f are respectively the mean value and the standard deviation calculated on the whole of the samples $(f_i)_{1 \le i \le N}$ of a function $f(x)$. *N* is the number of simulations of Monte Carlo.

The robust multi-objective optimization problem is thus built by simultaneously optimizing the original cost functions and their robustness:

$\begin{cases} M \text{in} F(x) = \left(f_1(x), f_1^r(x), ..., f_m(x), f_m^r(x)\right)^T \\ avec\ x \in S \end{cases}$ $f_i^r(x)$ is the robustness of the objective function $f_i(x)$ $i = 1, ..., m$.

The robust solutions with respect to uncertainties are those which simultaneously make it possible to minimize the original cost functions. $\left(f_1(x), f_2(x), ..., f_m(x)\right)$ and to maximize their robustness $\left(f_1^r(x), f_2^r(x), ..., f_m^r(x)\right)^T$

In this case we can study the cubic *nonlinear stiffness*.

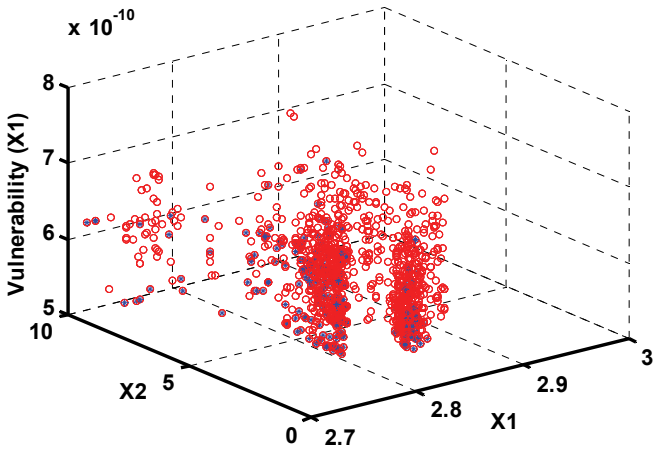

Fig. 27. r=3: Cubic nonlinear damping and stiffness – periodic motions: Overall solutions in space (X1, X2, Vulnerability (○) and robust solutions (*);.

Figure 27 illustrates the whole of the solutions obtained by simulation under the constraints given and in the band of sampling. Among these solutions one finds those which are robust (blue).

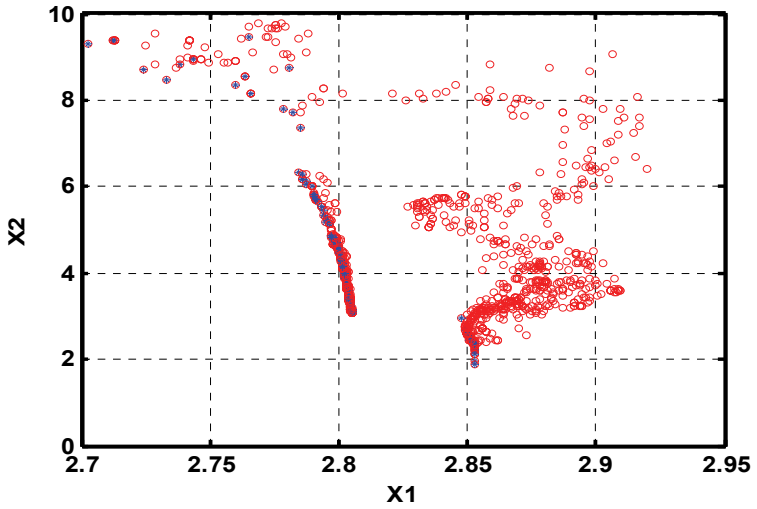

Fig. 28. Overall solutions in the plan (X1, X2) and robust solutions

Figure 28 presents the nonlinear displacement of the absorber according to the principal structure vulnerability. It is noted, that the designer has a flexibility to choose the absorber which is better appropriate with guarantee of robustness (minimal dispersion).
Figure 29 carries only the whole of the robust solutions in the plan X1 and X2. Figure 30 shows that the robust solution "A" which favours the minimal displacement of the absorber. The absorber maximum vibration is reduced to approximately 200%. This proves the importance of the proposed robust multi-objective optimization strategy in the periodic motions.

5. Conclusion

In this chapter, we proposed a mechanical system modeled by only one dof relating to its first mode and equipped with a dynamic absorber with only one dof too.
Thus the system obtained comprises a cubic and quadratic generalized nonlinearity combined stiffness and of damping. We used the numerical diagram of Newmark with linear acceleration in order to find the temporal response of the principal system with absorber subjected to a harmonic load.
Determinist calculations made it possible to highlight the contribution of this type of nonlinearity on the absorption of the vibrations and the behavior of the nonlinear system through the curves of phases (attractive, ovalization, etc).
The bifurcation diagram of the absorber in the cubic case for the chosen parameters illustrates three kinds of motions in several frequency bands: periodic, quasiperiod and chaotic motions.

In the optimization part, one determined the optimal characteristics of the damper located on the first face of Pareto with the compromise optimality-robustness. These solutions contribute to the robust design of the nonlinear system.

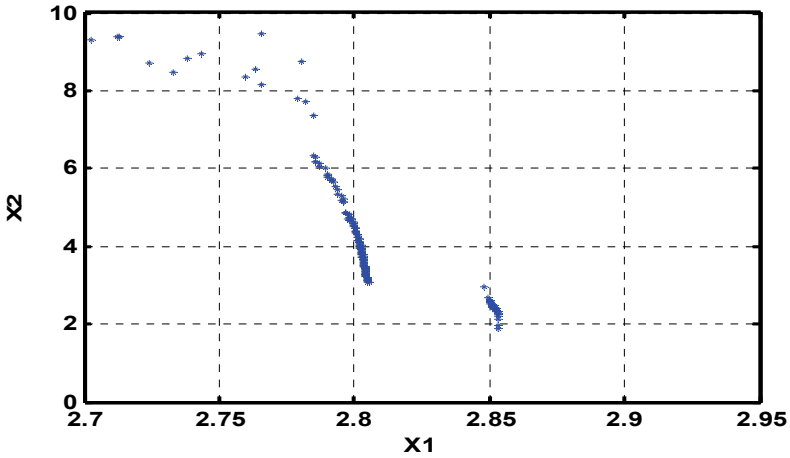

Fig. 29. Robust solutions in the plan (X1, X2)

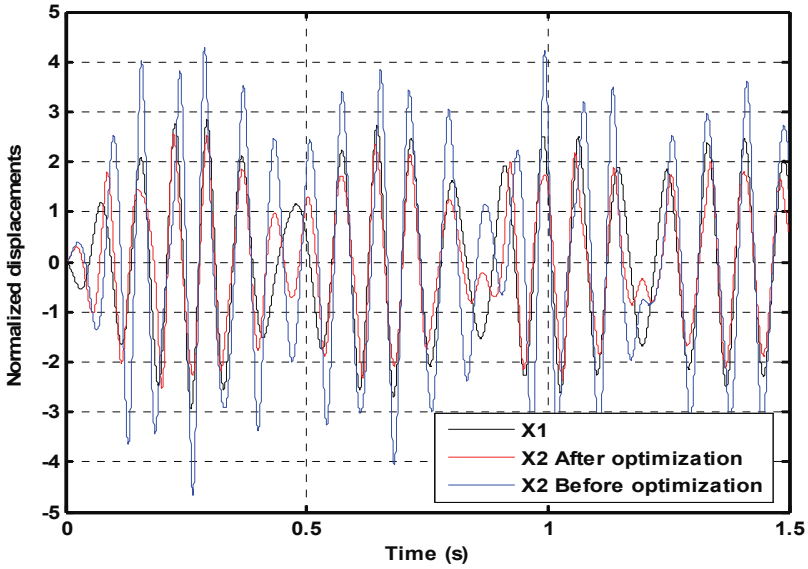

Fig. 30. Non-linear displacements before and after optimisation: Case of solution A

6. References

[1] G.S. Whiston, The vibro-impact response of a harmonically excited and preloaded one-dimensional linear oscillator, *Journal of Sound and Vibration* 115(2), pp. 303-319, 1987.

[2] S. Natsiavas, Steady state oscillations and stability of non linear dynamic vibration absorber, *Journal Sound and vibration* 156(2), pp. 227-245, 1992.

[3] S. Natsiavas, Stability of piecewise linear oscillators with viscous and dry friction damping, *Journal Sound and vibration*, Vol. 217, Issue 3, pp. 507-522, 1998.

[4] K.W. Chung, C. L. Chan, Z. Xu, J. Xu, A perturbation- incremental method for strongly non linear non autonomous oscillators, *International Journal of Non linear Mechanics*, 40, pp. 845-859, 2005.

[5] A.F. Vakakis and S.A Paipetis, the effect of viscously damped dynamic absorber on a linear multi-degree-of-freedom system, *Journal of sound and vibration*, vol. 105, Issue 1, pp 49-60 22 , 1986.

[6] S. Natsiavas, Dynamics of multiple-degree-of-freedom oscillators with colliding components, *journal of sound and vibration* 165 (3), 439-453 ,1993.

[7] S. Natsiavas and Tratskas P. On vibration isolation of mechanical systems with non-linear foundations *journal of sound and vibration*, volume 194, issue 2, 11 July 1996, p 173-185.

[8] G.Verros and S.Natsiavas, Forcing induced asymmetry on dynamical systems with cubic non linearity, *Journal of sound and vibration* volume 233, Issue 2, 1 June 2002, p 279-295.

[9] S.J.Zhu, Y.F Zheng and Y.M. Fu, Analysis of non-linear dynamics of a two-degree-of-freedom vibration system with non-linear damping and non linear spring, *Journal of sound vibration* 271, pp.3 15-24, 2004.

[10] B. Erkus, Comparison of the techniques used in the New mark analysis of non linear structures.*17th ASCE Engineering Mechanic conference June* 13-16, University of Delware Newmark de EM, 2004.

[11] D.Roy and R. kumar, A multi-step transversal linearization (MTL) method in non-linear structural dynamics, *journal of sound and vibration* 287, pp. 203-226, 2005.

[12] A.F.EL-Bassiouny, Effet of non linearities in elastomeric material dampers on torsional oscillation control, *Applied Mathematics and Computation* 162 (2005) 835-854.

[13] D. Schaffer, Multiple Objective Optimisation with Vector Evaluated Genetic Algorithm, In genetic algorithm and their applications, *Proceedings of the First International Conference on Genetic Algorithm*, pp. 93-100, 1985.

[14] E. Zitzler and L. Thiele, Multiobjective Evolutionary Algorithms: A comparative case study and the strength Pareto approach, *IEEE Transaction on evolutionary computation*, vol. 3, pp. 257-271, 1999.

[15] N. Srivinas, K. Deb, Multiobjective Optimisation using Non dominated Sorting in Genetic Algorithms, *Technical Report*, Department of Mechanical Engineering, Institute of Technology, India, 1993.

[16] M.- L. Bouazizi, S. Ghanmi, R. Nasri, N. Bouhaddi, Robust optimization of the non-linear behaviour of a vibrating system, *European Journal of Mechanics*-A/Solids, volume 28 (2009), pp: 141- 154.

[17] S. Ghanmi, M.-L. Bouazizi, N. Bouhaddi, Robustness of mechanical systems against uncertainties, 24rd, *Finite Elements in Analysis and Design* 43(2007), pp. 715 – 731.

[18]B. Ait Brik , S. Ghanmi, N. Bouhaddi, S. Cogan, Robust Multiobjective optimisation Using Response Surfaces, 23 rd, *International Modal Analysis Conference* (IMAC-IVX), orlando, USA,Inc., 2005.

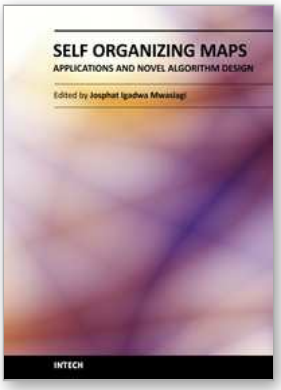

Self Organizing Maps - Applications and Novel Algorithm Design
Edited by Dr Josphat Igadwa Mwasiagi

ISBN 978-953-307-546-4
Hard cover, 702 pages
Publisher InTech
Published online 21, January, 2011
Published in print edition January, 2011

Kohonen Self Organizing Maps (SOM) has found application in practical all fields, especially those which tend to handle high dimensional data. SOM can be used for the clustering of genes in the medical field, the study of multi-media and web based contents and in the transportation industry, just to name a few. Apart from the aforementioned areas this book also covers the study of complex data found in meteorological and remotely sensed images acquired using satellite sensing. Data management and envelopment analysis has also been covered. The application of SOM in mechanical and manufacturing engineering forms another important area of this book. The final section of this book, addresses the design and application of novel variants of SOM algorithms.

InTech Europe
University Campus STeP Ri
Slavka Krautzeka 83/A
51000 Rijeka, Croatia
Phone: +385 (51) 770 447
Fax: +385 (51) 686 166
www.intechopen.com

InTech China
Unit 405, Office Block, Hotel Equatorial Shanghai
No.65, Yan An Road (West), Shanghai, 200040, China
中国上海市延安西路65号上海国际贵都大饭店办公楼405单元
Phone: +86-21-62489820
Fax: +86-21-62489821